



A high-resolution perspective of extreme rainfall and river flow under extreme climate change in Southeast Asia

Mugni Hadi Hariadi^{1,2,3}, Gerard van der Schrier¹, Gert-Jan Steeneveld², Samuel J. Sutanto⁴, Edwin Sutanudjaja⁵, Dian Nur Ratri³, Ardhasena Sopaheluwakan³, and Albert Klein Tank⁶

¹Royal Netherlands Meteorological Institute (KNMI), De Bilt, Netherlands

²Meteorology and Air Quality, Wageningen University and Research (WUR), Wageningen, Netherlands

³Indonesian Agency for Meteorology, Climatology and Geophysics (BMKG), Jakarta, Indonesia

⁴Water System and Global Change, Wageningen University and Research (WUR), Wageningen, Netherlands

⁵Utrecht University, Utrecht, Netherlands

⁶Met Office Hadley Centre for Climate Science and Services, Exeter, United Kingdom

Correspondence: Mugni Hadi Hariadi. Royal Netherlands Meteorological Institute (KNMI) Utrechtseweg 297, 3731 GA De Bilt (Email: mugni.hariadi@knmi.nl; mugni.hariadi@bmkgo.id; mugnihadi@gmail.com)

Abstract. This article provides high-resolution information on the projected changes in annual extreme rainfall and high and low streamflow events over Southeast Asia under extreme climate change. The analysis was performed using the bias-corrected result of the High-resolution Model Intercomparison Project (HighResMIP) multi-model experiment for the period 1971-2050. Eleven rainfall indices were calculated along with streamflow simulation using the PCR-GLOBWB hydrological model. The historical period 1981-2010 and the near-future period 2021-2050 were considered for this analysis. Results indicate that over Indochina, Myanmar faces more challenges in the near future. The east coast of Myanmar will experience more extreme high rainfall conditions, while northern Myanmar will have longer dry spells. Over the Indonesian maritime continent, Sumatra and Java will suffer from the increase in dry spell length of up to 40%, while the increase of extreme high rainfall will occur over Borneo and mountainous areas in Papua. Based on the streamflow analysis, the impact of climate change is more prominent in a low flow event than in a high flow event. The majority of rivers in the central Mekong catchment, Sumatra, the Malaysian peninsula, Borneo, and Java will experience more extreme low flow events. More extreme dry conditions in the near future are also seen from the increasing probability of future low flow occurrences, which reaches 101% and 122% on average over Sumatra and Java, respectively. Finally, the changes in extreme high and low streamflow events are more pronounced in rivers with steep hydrographs, while rivers with shallow hydrographs have a higher risk in the probability of low flow change. Our study highlights the importance of catchment properties in aggregating and/or buffering the impact of extreme climate change.

1 Introduction

The IPCC's sixth assessment report (IPCC6AR) indicates that Southeast Asia (SEA) is one of the most vulnerable regions to climatic changes and thus is highly exposed to the impacts of climate change (IPCC, 2021). Smit and Wandel (2006) explained that vulnerability is usually considered to be the product of three elements: exposure, sensitivity, and adaptive capacity. One of the challenges SEA faces is that climate change leads to increasing extreme rainfall, and this condition is aggravated by



the low resilience and adaptive capacity of most developing countries in SEA (Hijioka et al., 2014). Besides extreme rainfall events, sea level rise, drought, high temperatures, and the resulting increasing scarcity of freshwater, loss of biodiversity, and other aspects of environmental degradation are the results of climate change that have negative impacts on Southeast Asian economies and societies Jasperro and Taylor (2008). The climate change vulnerability mapping for SEA has been documented
25 by Yusuf and Francisco (2009). Those extreme events, especially extreme rainfall, are projected to intensify in the future under climate warming (Ali and Mishra, 2017).

Several previous studies documented the observed changes in climate in the SEA region (Supari et al., 2017; Siswanto et al., 2016; Suhaila et al., 2010; Cinco et al., 2014). Supari et al. (2017) found a tendency towards wetter conditions by looking at the simple daily precipitation intensity (SDII), a significantly increasing trend in the annual highest daily rainfall amount
30 (RX1day), and the rainfall amount contributed by the extremely very wet days (R99p). In addition, Siswanto et al. (2016) observed trends in extreme rainfall over Jakarta - Indonesia and found that the number of days with rainfall exceeding 50 and 100 mm per day shows a statistically significant increase from 1961 to 2010. They added that the trends in extremes are strongest during the wet season compared to the dry season. For the Malaysian Peninsula, Suhaila et al. (2010) studied trend patterns during the wet and dry seasons and they found a decrease (increase) in total rainfall and a significant decrease
35 (increase) in the frequency of wet days leading to a significant increase in rainfall intensity during the southwest (northeast) monsoon over most of the region. Moreover, In Thailand, Limsakul et al. (2010) revealed changes in rainfall extreme events along Thailand's coastal zones in recent decades observed from three different stations; Andaman Sea Coast (ASC), the Gulf of Thailand's western coast (GoTw), and the Gulf of Thailand's eastern coast (GoTe). These authors found an overall decrease in total rainfall amounts accompanied by a coherent reduction of heavy and intense rainfall events in ASC, and more intense
40 daily rainfall associated with a significant decrease in the number of rainy days in GoTw. However, in GoTe, the changes in extreme precipitation were relatively mixed between significant positive and negative trends. In addition, Cinco et al. (2014) observed an increase in extreme events over 34 synoptic weather stations in the Philippines for the period 1951-2010 compared to the normal mean values for the period 1961-1990.

The variations and changes in precipitation extremes in SEA become a crucial factor for several sectors of life, e.g., the
45 agricultural sector when addressing food security issues (Knox et al., 2012; Lin et al., 2022; Redfern et al., 2012), economics (Weiss et al., 2009), and the hydrological sector (Hoang et al., 2016). Hydrology plays an important role in meeting the grand challenges of many sectors, such as availability of fresh water, food security, supply of water to hydropower facilities, the vitality of ecosystems, sanitation and sustainable development (Singh and Xiaosheng, 2019). A state-of-the-art hydrological model becomes an essential tool for the effective planning and management of water resources and recently, research has
50 broadened to include sustainable water in relation to climate change-induced changing patterns of streamflow. A decrease in streamflow for such a long period may cause drought that can trigger impacts on the water supply, energy, water-borne transportation, and ecosystems (Stahl et al., 2016). Studying this can help decision-makers in managing the river basin as a key factor affecting the volume of water required to cope with the increasing demands of the population and several specific activities such as agriculture, energy, and tourism sectors, which directly depend on water resources (Mair and Fares, 2010).



55 To uncover the cause of hydrological drought from a perspective of climate change, it is important to investigate the links
between rainfall-related climate indices and hydrological drought, which can help in identifying future drought events (Huang
et al., 2016). As precipitation is the key factor controlling streamflow and hydrological response in catchments (Lobligeois
et al., 2014), an approach based on assessing precipitation changes and hydrological changes is called for. Climate indices
are simple diagnostic quantities that can be used to describe the state changes in the climate system. Examples are the many
60 impact-relevant indices to measure precipitation changes and variation from the Expert Team on Climate Change Detection
Indices (ETCCDI) (Klein Tank et al., 2009). For scientific and operational purposes, exploring the space-time variability of
hydrologic extremes in relation to climate is important (Renard and Thyer, 2019). Renard and Thyer (2019) study shows that
climate indices have frequently been used as predictors to describe hydrologic extremes.

Understanding past, present, and future climate change, the Southeast Asia Regional Climate Downscaling / Coordinated
65 Regional Climate Downscaling Experiment (SEACLID/CORDEX-SEA) (<http://www.ukm.edu.my/seaclid-cordex>) group has
dynamically downscaled a multi-model of the Coupled Model Intercomparison Project Phase 5 (CMIP5) into a high-resolution
dataset (Cruz et al., 2017; Juneng et al., 2016; Ngo-Duc et al., 2017). Based on the output of the experiment, the previous stud-
ies show the increasing risk of drought and extreme rainfall over the region (Ngai et al., 2020a, b; Nguyen-Ngoc-Bich et al.,
2021; Supari et al., 2020; Tangang et al., 2018, 2019; Trinh-Tuan et al., 2019). Utilizing the same dataset, other studies have
70 already focused on some rivers in Malaysia to show the impact of climate change on the hydro-meteorological droughts (Tan
et al., 2019, 2020). Although climate change's impact on hydroclimatic extremes over SEA has been previously studied espe-
cially by the CORDEX-SEA group, the use of the latest version of high-resolution CMIP for this topic is still limited. The
previous studies show the CMIP6 high-resolution Modeling Intercomparison Project (HighResMIP) (Haarsma et al., 2016)
result simulated closer monsoon characteristics (Hariadi et al., 2021) and rainfall indices (Hariadi et al., 2022) to observation
75 than CMIP5 downscaled result from CORDEX-SEA.

In this study, we aim to use HighResMIP model results (Haarsma et al., 2016) to investigate the change of extreme rainfall
and its impact on river flow under extreme climate change in the near future period over SEA. A bias-corrected of HighResMIP
is constructed to look at the changes in climate indices, in this case; rainfall indices and investigate the change and the trend
of the indices. This dataset is then used to simulate the river streamflow over four domains in the SEA region i.e., the Mekong
80 basin, Sumatra-Malaysian peninsula, Java, and Borneo. Furthermore, the changes in streamflow values during low flow and
high flow events and their probability in the near future are investigated.

2 Material and Methods

2.1 Description of the study area

The Southeast Asia domain (SEA) used in this study is located between 14.8°S - 34°N and 89.5°E - 146.5°E. This includes the
85 Indonesia maritime region in the South, the Philippine maritime region in the East, and Indochina (South of China, Myanmar,
Thailand, Laos, Cambodia, Vietnam and Malaysia peninsula) in the Northwest. This domain covers the Mekong basin in the
North SEA. The mountain region over Southern China to northern Laos is part of the upstream part of the Mekong rivers.



On the maritime continents, mountain ranges are spread from the Philippines to islands in Indonesia, such as Sumatra, Java, Sulawesi, and Papua. These mountains specify the streamflow characteristics in the regions.

90 The rainfall in these regions is dominated by the monsoon season which starts from the North SEA in May and moves to the South SEA in November (Aldrian and Susanto, 2003; Hamada et al., 2002; Hariadi et al., 2021; Moron et al., 2009). Some areas in the SEA, such as Myanmar (Li et al., 2013), Vietnam (Nguyen-Thi et al., 2012; Luu et al., 2021) and Philippine (Corporal-Lodangco and Leslie, 2017) are affected by tropical cyclones, which lead to high extreme precipitation.

2.2 Data

95 2.2.1 Climate data

Our study uses the climate model output from the high-resolution model intercomparison project (HighResMIP) (Haarsma et al., 2016) that is available from the H2020-funded Primavera project (Roberts et al., 2020). This model has a spatial resolution (25-50km spatial resolution) comparable to the downscaled output of the regional climate model (RCM) which is based on the coupled model intercomparison project phase 5 (CMIP5) over SEA (CORDEX-SEA). Previous studies show that the HighResMIP has a better simulation of the monsoon characteristics (Hariadi et al., 2021) and extreme precipitation (Hariadi et al., 2022) than the CORDEX simulations over SEA when compared against the observational SA-OBS (Van den Besselaar et al., 2017), APHRODITE (Yatagai et al., 2012) and CHIRPS (Funk et al., 2015) observational datasets. We use the coupled historic runs of the HighResMIP for the historical period 1950-2014 (Hist-1950) and the future period 2014-2050 (high-res-100 future). Compared to the historically forced atmosphere run of HighResMIP (HighResSST), the Hist-1950 shows similar performance on simulating the monsoon characteristic (Hariadi et al., 2021) and the extreme precipitation (Hariadi et al., 105 2022) over SEA. This shows the high skill of the ocean model in the coupled models. We used five models that are available from the coupled models of HighResMIP, which are the CMCC (Cherchi et al., 2019), CNRM (Voltaire et al., 2019), EC-Earth (Haarsma et al., 2020), HadGEM (Roberts et al., 2019) and MPI (Müller et al., 2018). Only one member is available for the CMCC, CNRM and MPI model simulations, while EC-Earth and HadGEM have four and three members available.

110 2.2.2 Streamflow data

Global hydrological models (GHMs) have been developed over the last decade and become essential tools to quantify the global water cycle. The GHMs simulate distributed hydrological responses to climate and weather variations at a higher resolution than what is possible in general circulation models (GCMs). One of the recently developed GHMs is a grid-based global hydrological model called PCR-GLOBWB (PCRaster Global Water Balance) (Van Beek et al., 2011; van Beek et al., 2012). 115 PCR-GLOBWB describes the terrestrial part of the hydrological cycle that focuses on global water availability issues (Van Beek et al., 2011; van Beek et al., 2012). Sutanudjaja et al. (2018) added more advanced run-off processes, river routing, and groundwater components to this model i.e., PCR-GLOBWB 2.0 and extensively evaluated its performance.

We used the PCR-GLOBWB 2.0 (Sutanudjaja et al., 2018; Trambauer et al., 2014; Sperna Weiland et al., 2010) in this study to simulate historical and future streamflows. This model is available in two resolutions; a 5-arcminute and in a 30-arcminute



120 resolution. This model simulates the terrestrial water balance on a daily time step. Sutanudjaja et al. (2018) described the
parameters, the standard input data, and the parameterisation of this model. The parameterization for PCR-GLOBWB 2.0 is
mostly the same as the one for PCR-GLOBWB 1.0 (Bierkens and Van Beek, 2009). There are 5 modules in the PCR-GLOBWB
2.0: the meteorological forcing, the land surface, the groundwater, the surface water routing, and the irrigation and water use
that are calculated in a daily time step (Ruijsch et al., 2021). In this study, we use configuration as in Sutanudjaja et al. (2018).
125 The difference is that in our study we exclude the water used factor and focus more on meteorological exposure. The model
runs in 5 arcmins spatial resolution, which is about 10 km by 10 km at the equator. We simulated daily water discharge for
the period of 1971-2050, based on bias-corrected model data using the PCR-GLOBWB hydrological model. A conservative
remapping method was used to interpolate the bias-corrected climate data models into 5 arcmins spatial resolution. Rainfall
and the air temperature were used as input, while the potential evapotranspiration was estimated using the Hamon method
130 (Hamon, 1961). To simulate a better fluctuation of daily streamflow, we selected the kinematic wave for the routing method.

The simulation was run for four domains, they are the Mekong basin (MEB), the Sumatra-Malaysia basin (SMB) and the
islands of Java and Borneo. Based on the evaluation of PCR-GLOBWB 2.0 simulation using streamflow data from the Global
Runoff Data Centre (GRDC), the model show correlation and Kling-Gupta Efficiency coefficient or KGE (Gupta et al., 2009)
values range between 0.21 to 0.98 and -6.49 to 0.87 for MEB (137 observation sites), 0.29 to 0.70 and -2.51 to 0.41 for SMB
135 (14 observation sites), 0.16 to 0.80 and -1.98 to 0.34 for Java island (10 observation sites) also 0.36 to 0.70 and 0.07 to 0.34 for
Borneo island (5 observation sites) (Sutanudjaja et al., 2018). This indicates that the model has good performance to simulate
the observed streamflow in many river basins across SEA.

2.3 Methods

2.3.1 Climate Indices

140 In this study, we used 11 rainfall-related climate indices, which were earlier used to assess the realism of model simulations
(Hariadi et al., 2022). The indices were calculated using the package developed by Schulzweida and Quast (2015), which is part
of the climate data operator (CDO) suite of routines (Schulzweida et al., 2006). Nine indices were adopted from the ETCCDI
team (Klein Tank et al., 2009). In addition, we also calculated the number of consecutive dry days periods (CDD) and consec-
utive wet days periods (CWD) exceeding five days (CDD5D and CWD5D) that are available in the package (Schulzweida and
145 Quast, 2015). The indices are aggregated to the annual level. The percentile value for the rainfall fraction due to very wet days
(exceeding the 95th percentile) (R95pTOT) is calculated based on the 1971-2050 period. Table 1 lists names and definitions of
the rainfall-related climate indices computed in this study.

2.3.2 Bias Correction

The global circulation model is handicapped by biases to the degree that prevents their direct use for hydrological purposes
150 (Ehret et al., 2012). Earlier studies discussed the biases in the CMIP5 model simulation (e.g., Taylor et al., 2012), where the



bias is worse for precipitation simulation over regions with complex topography (Mehran et al., 2014). Ngai et al. (2017) discussed the need for bias correction on precipitation and temperature simulation of regional climate models over SEA.

Empirical quantile mapping (EQM) is one of the bias correction methods that is widely used. The number of quantiles in this method is a free parameter Piani et al. (2010). Previous studies used the EQM as a quantile-quantile calibration method based on a nonparametric function that corrects biases in the cumulative distribution functions (CDFs) of climatic variables (Boé et al., 2007; Amengual et al., 2012). Recently, Fang et al. (2015) compared bias correction methods in downscaling meteorological variables for a hydrologic impact study in China, Ratri et al. (2019) used EQM to bias-corrected ECMWF SEAS5 over Java island, Indonesia and Hariadi (2017); Ngai et al. (2017); Amsal et al. (2019) used quantile mapping to bias-corrected RCM simulation over SEA.

EQM works with empirical probability density functions (PDFs) or CDFs for forecasts and observations. This method attempts to correct the distribution of the GCM and RCM simulated data so that it matches the distribution of the observational dataset (Déqué et al., 2007; Block et al., 2009). EQM estimates quantiles for the forecast and the observation dataset and forms a transfer function by using corresponding quantile values. Then, each predicted quantile is substituted by the corresponding observed quantile using their Empirical CDFs (ECDFs). The transfer function is then applied to the forecast data as follows.

$$Y_{f(bc)} = ECDF_o^{-1}[ECDF_f(Y_f)]$$

where Y_f is the raw precipitation forecast, and $Y_{f(bc)}$ is the bias-corrected precipitation re-forecast. $ECDF_o$ is the inverse ECDF of the observations, and $ECDF_f$ is the ECDF of the forecast values.

We used the rainfall and temperature gridded dataset obtained from the APHRODITE (Yatagai et al., 2012) as the observation (reference data) in the bias correction. The reference period for the bias correction is 1971-2010. For rainfall, the APHRODITE V1101 for the period of 1971-2006 was combined with the APHRODITE V1101 EXR1 for the period of 2007-2010. Whereas for the temperature, we use APHRODITE V1808. Limited gauge density and availability of long-term climatological data make the development of a dataset for daily precipitation amounts based on in-situ measurements challenging (Van den Besselaar et al., 2017; Singh and Xiaosheng, 2019). The Southeast Asia Observation dataset (SA-OBS) (Van den Besselaar et al., 2017) developed especially for SEA has the highest density of gauges than other datasets available. However, limited coverage of SA-OBS is not cover the entire Mekong basin. This is the reason we used APHRODITE for this study. Hariadi et al. (2022) found that both APHRODITE and SA-OBS that developed from gauge data have more similarities than between both datasets with the Climate Hazards Group Infrared Precipitation with Stations v2.0 (CHIRPS; Funk et al., 2015) which is based on satellite data.

Figure 1 and S01 shows the results from the two-sample Kolmogorov–Smirnov test (K-S) of the original and bias-corrected model. It shows that the K-S statistic is lower for the bias-corrected simulation compared to the original (uncorrected) model. This indicates that the probability distribution of the bias-corrected model is closer to the observations compared to the uncorrected model for simulating these climate indices. More improvements are shown in the model simulation of climate indices that are directly related to rainfall intensity (R10mm, R20mm, Rx1day, Rx5day, R5day50mm and SDII) than other indices



that are more climatological (CDD, CDD5D, CWD, CWD5D and R95pTOT). Hariadi et al. (2022) also found that the model poorly simulates climate indices that are directly related to rainfall intensity. Based on the K-S value, we find a significant improvement in the model simulation on these climate indices after the bias correction was performed. Here, we show the importance of the bias-correction process for model simulation on climate indices. This study, therefore, uses the bias-corrected dataset for further analysis.

2.3.3 High and low flow indices

The high and low flow indices were identified using the threshold-based approach. This approach applies the theory of runs and is developed based on a pre-defined threshold level for each index (Yevjevich, 1967; Hisdal et al., 2004; Sutanto and Van Lanen, 2021). Thresholds in this study were derived from the 10th and the 95th percentiles of the daily streamflow (Q10 and Q95 of flow duration curve), which are the flows that are either equal or lower than 10 percent of the time or exceeded 95 percent of the time. We calculated both the 10th and the 95th percentiles of the daily discharge for the combined historical and the near future periods. The 10th percentile represents low flow discharge (LFD) (Tallaksen et al., 1997; Wong et al., 2011), while the 95th percentile identifies high flow discharge (HFD) (van Vliet et al., 2013; Asadieh and Krakauer, 2017). We investigate the change of LFD and HFD in the near future period (2021-2050) compared to the historical period (1981-2010). A decrease in LFD indicates that the driest 10% of daily discharges are drier than those for the historical period, whereas an increase in HFD indicates more severity of the 5% most extreme high discharge events. Using the 10th and 95th percentiles of the historical period as a reference of extreme events, we calculate the probability change of the extreme low and extreme high events in the near future. The increase in the probability indicates that events considered extreme in the historical period will occur more frequently in the near future.

3 Results

3.1 Change in climate indices over Southeast Asia

The climate indices (Table 1) for the period 1971-2050 from the bias-corrected models were calculated to show the change in extreme rainfall. We calculated the change of climate indices between the near-future period (NF, 2021-2050) and the historical period (Hist, 1981-2010). In addition, we also calculated the trend over the period 1971-2050 including the Sens slope significance test with a 95% confident level (Sen, 1968). The final change of climate indices value is based on the model mean, this has some uncertainty of extreme value that might be shown by some of the models. While in the trend significance test, the final result is based on the model agreement, which is not affected by the extreme value that might be shown by some of the models. The trend is considered significant when 3 or more out of 5 models (60%) show a significant result. For EC-Earth and HadGEM, which have 4 and 3 members respectively, the trend is considered significant when at least 3 or 2 members show a significant trend.



Figure 2a shows increasing CDD over some areas in the Philippines, the northern part of Myanmar, the southern part of Vietnam and Thailand, Cambodia, and the centre of the Malaysian peninsula. Over the Indonesian region, an increase between 20% to 40% is seen in the Southern part of Sumatra. The increase of CDD is also found in Java, Bali, Nusa Tenggara, the Southern part of Borneo, and the Northern part of Sulawesi. Similar to the change in Indochina and the Philippines, the increase is less than 20% in most of these areas. In addition, there is also a decrease of CDD in the mountains region of Papua up to 15%. We found a robust signal of increasing CDD over the northern part of Myanmar, the southern part of Sumatra, and some areas in Java which not only show the increasing change of CDD value but also show a significant trend up to 3 days/decade (Fig. 2a). The drier condition in the near future over the Southern part of Sumatera is also shown by the increasing CDD5D over the region, with a significant increasing trend of CDD5D (Supplementary Material Fig. S2). Most of the areas that may experience higher CDD and CDD5D in SEA also show a decrease in CWD and CDD5D (Supplementary Material Fig S3 and S4).

The change in frequency of heavy rainfall events (precipitation events with daily amounts greater than or equal to 20 mm (R20mm)) in the near future compared to the historical period is also apparent in our result (Figure 2a). Northwestern Indochina and several islands in the maritime continents, such as Sumatra, Borneo, Sulawesi, and Papua are projected to have an increase of R20mm. A high increase (>40%) of R20mm is found over some areas in the Eastern part of Borneo and mountainous areas in the northern part of Papua. Based on a model agreement, a significant increasing trend for both R20mm and R10mm also appears over Borneo and the mountainous area in northern Papua (Fig. 2b and S5b). This clearly indicates a robust signal of increasing heavy and very heavy rainfall events over those regions.

The change in intensity of yearly maximum one-day precipitation (Rx1day) is depicted in Figure 2c. Rx1day shows an increasing intensity scattered over Indochina, especially in the west coast and the northern part of Myanmar, the west and east coast of the Malaysian peninsula, and some areas in Thailand, Cambodia, and the southern part of Vietnam. Over the Indonesian region, Rx1day increases over Borneo, Sumatra, Sulawesi, and mountainous areas over Papua. A similar pattern is also found for the maximum 5-day precipitation (Rx5day) as shown in Supplementary Figure S6a. Although Rx1day and Rx5day exhibit increasing trends spreading over SEA, the trends are stronger over the west coast of Myanmar and the mountainous area of Papua (Fig. 2c and S6b).

The change in the rainfall fraction due to extreme wet days (exceeding the 95th percentile) (R95pTOT) is shown in Figure 2d. The figures clearly indicate an increase of R95pTOT across SEA. In the near future, large percentages of areas with an increase in R95pTOT are found over west northern, and central Indochina, Malaysia peninsula, Sumatra, Borneo, Sulawesi, and Papua. Especially over the west coast of Myanmar, Borneo, and Papua, there is a high increase of R95pTOT (>20%). In terms of the model agreement on the trend significance, a significant increase in trend is found over west northern Indochina, Borneo, and the mountainous region in Papua.

Regarding the Simple Daily Intensity Index (SDII), Figure 2e shows an increase of SDII (>10%) over the western part of Myanmar, the east coast of the Malaysian peninsula, northern Philippines, Borneo, and Papua. A significant increasing trend of SDII is seen over the northern Philippines, Southern Sumatra, Sulawesi, Borneo, Papua, and some areas in Indochina. Over



250 Malaysia peninsula, a significant positive trend is found over the west coast of the Malaysia peninsula instead of the east coast of the region, which has a higher increasing value of SDII.

3.2 Change in streamflow over Southeast Asia

Streamflow is the volumetric flow rate of water per unit of time that is transported through a given river cross section. Figures 3a and 3b indicate the percentage of LFD change and the percentage of change in the probability of extreme low flow over
255 MEB. Figures 3c and 3d show the percentage of HFD change and the percentage of change in the probability of extreme high flow over MEB. The decreasing (increasing) of LFB (HFD) indicates the more extreme condition of low (high) flow events in the near future. Figures 3 a and b show that future low flows will be more severe and the probability for low flows increases, these conditions spread more over the central and southern parts than over the northern part of MEB. Over 76% area of MEB will face decreasing in LFD (16% decrease on average), with 15% of this area showing a decrease in more than 25% LFD.
260 In terms of low flow events, the majority area of the region (82%) shows an increasing probability with a 66% increase (on average). Moreover, 72% from this area will experience a sharp increase of greater than 25%. A Significant decreasing LFD and increasing probability of low flow events appear in the centre part of MEB (25°N - 17°N), with 23% and 104% on average.

In terms of high discharge, half of the region shows an increase in HFD (50% area) (Fig. 3c) and probability of high flow events (49% area) (Fig. 3d) in the near future. However, the magnitude for both indices is relatively low with only a 5% and
265 12% increase on average, respectively for HFD and probability of high flow events. Slightly in contrast to the low flows, more extreme condition of high flow shows over the northern part of the region.

The percentage of LFD and HFD change and the probability change in extreme low and high flows in SMB are shown in Figure 4. Figures a and b show that future low flows will be more severe and the probability of low flows increases. Over 91% of SMB will see further reductions of flow with (on average) 19% but peaking area to average decreases of 22-24% for the
270 central (2°S - 2°N) and southern (below 2°S) parts Sumatra island. These are higher than the northern part of Sumatra and the Malaysian peninsula with (on average) 17% and 15% decreases. Furthermore, the probability of extreme low flow events will increase over 94% of SMB (101% on average), with 95% of these areas experiencing an increase in the probability of more than 25% compared to the historical (Fig. 4b). Over Sumatra, all parts of the island show increasing probability with (on average) 146%, 127%, and 76% increases for the northern, central, and southern parts, respectively. While the Malaysian
275 peninsula, the average increase in the probability of extreme low flow events reaches 73%.

In contrast to the low flows, the high flows will get less extreme (Fig. 4c) and the probability of high flows is insignificantly increasing (Fig. 4d) over the SBM region. In terms of high flow, 49% of SMBs show increasing HFD in the near future. On average, the increasing HFD is only 7% across SMBs. Compared to other areas in the region, the increasing high discharge is more prominent in the Malaysian peninsula with 70% of this region showing a higher HFD of 10% on average than in the past.
280 In terms of High flow events, 59% of the region shows an increased probability of the events with an average 19% increase.

In Java Island (Fig. 5), the increasing severity during low flow events in the near future is higher than the increasing severity during high flow events. The decreasing LFD will occur over a large area of Java (85%) (Fig. 5a). The average value of the decrease in LFD is 13%. Although the percentage area that shows decreasing LFD over the western part (79%) is less compared



to the eastern part (96%) of Java, the magnitude of the decreasing LFD is higher for the western part. The average decreasing
285 LFD for the western and eastern parts of Java are 19% and 8%, respectively. A slightly different condition is shown in the
probability of extreme low flow event compared to low streamflow change over Java (magnitude). The increasing probability
of extreme low flow events is more pronounced in the eastern region (126% on average from 98% of the areas having higher
probability) compared to the western region (52% on average from 90% of the areas having higher probability) (Fig. 5b). The
increase of high flow magnitude over Java is lower than the low flow. 58% of Java shows an increasing HFD in the near future
290 (Fig. 5c). However, the maximum increase of HFD in the Java island is only 11%, with 3% as an average. In general, the
increasing HFD is relatively low in Java unlike other locations in SEA. The increase in the probability of extreme high flow
events is more significant compared to the increase of HFD (Fig. 5d). A large part of Java (75%) will experience an increase in
probability, with 25% of these areas indicating a higher probability of >25% in the future. The average of increasing probability
is 16% across Java.

295 In Borneo, both high and low flow events are projected to increase in near future, especially in terms of the probability of
change in extreme events. Here, even though it is projected that 91% of the area will experience lower LFD in near future,
the magnitude is relatively low, which is only a 10% decrease in LFD on average (Figure 6a). The decreasing LFD over the
southwest part of Borneo is more than in the other parts of the island. On the contrary with the relatively little decrease in low
streamflow, the increase in the probability of extreme low events over Borneo is fairly significant. Figure 6b shows that the
300 increase in the probability of low flow events will occur in 94% of Borneo Island, with 74% of these areas will experience a
higher probability of >25%. In addition, the entire southern part of Borneo will experience an increasing probability of low
flow events, which is divided into the southwestern part (67% increase on average) and the southeastern part (59% increase on
average).

Figure 6c shows a percentage of HFD changes in Borneo. It shows that most of the region (89%) will experience increasing
305 HFD, spreading more from the northwest to the southeast. However, the increasing HFD is relatively low, with an average
of 8%. Figure 6d demonstrates that the increase in the probability of extreme high flow events occurs over 90% of Borneo,
spreading more from the northwest to the southeast. The average increase in probability is 28%, with almost half of the
increased probability being >25% in the near future.

4 Discussion

310 4.1 Extreme climatic changes

Compared with the previous study by the Coordinated Regional Climate Downscaling Experiment – Southeast Asia (CORDEX-
SEA) group, we found some similarities and some differences in our results. Tangang et al. (2018) found that Myanmar will
have more consequences of extreme events due to global warming than other regions in Indochina. Northern Myanmar will
experience more severe extreme dry and wet conditions in the future under the 2°C global warming scenario. This is confirmed
315 in our results where we found that the northern part of this region shows an increasing dry spell length (CDD) and the models
show an agreement on the increasing trend of CDD in the near future, indicating that this increase is a robust signal. In ad-



dition, the western coast of this region will also experience higher precipitation extremes, as indicated by some indices, such as Rx1day, Rx5day, R95pTOT, and SDII. The contrasting behaviour between longer dry periods and more intense rainfall is a trend that is observed globally as well (Benestad et al., 2022). Tangang et al. (2019) found that Thailand will experience wetter conditions over the northern-central-eastern parts and drier conditions over the southern part. A similar pattern of index changes was also found in this study. However, based on the model agreement, we found no significant trend in these wet and dry conditions. Nguyen-Ngoc-Bich et al. (2021) found that based on Palmer Drought Severity Index, substantial increases in drought duration, severity, and intensity appear over northern parts of the North Central sub-region, parts of the Central Highlands and over southern Vietnam. In our study, we could only confirm that longer dry spells (CDD) appear over the east coast of the Southern part of Vietnam, but there is no model agreement on the trend significance.

Ngai et al. (2020a) demonstrated that rainfall extremes are likely to decrease (increase) over the Malaysian peninsula (Malaysian Borneo) by the end of the century. However, our result is contradicting in the sense that an increase in extreme rainfall is seen over the Malaysian peninsula although the increase is less than in Malaysian Borneo. Some decreases in the number of heavy precipitation days (R10mm) are projected over some areas in the Malaysian peninsula but this decrease is not clear for other extreme rainfall indices. In addition, Ngai et al. (2020b) found high increases of R20mm, RX1day, R95pTOT, and R99pTOT, and also small increases in SDII and CDD over the Malaysia region. Our study yields similar conditions for those parameters except for SDII which shows a high increase. The increase of SDII spreads over the region and shows a significant trend over the western part of the Malaysian peninsula and the majority of Malaysian Borneo.

A previous study by Supari et al. (2020) found that the increase of CDD is higher than the increase of Rx1day and frequency of extremely heavy rainfall (>50mm) (R50mm), especially over the Indonesian region. Accordingly, Tangang et al. (2018) also simulated a robust increase in CDD, which indicates drier conditions over Indonesia in the future. The almost similar conditions between CDD and Rx1day are found in our study. Although the increase of Rx1day is scattered over SEA, the increasing CDD is more prominent than Rx1day, especially in the Indonesian region. In our study, we also calculated R20mm instead of R50mm, which slightly shows a different result. The increase of R20mm is more prominent than CDD. Over the Indonesia region, a significant increasing trend of R20mm appears over Borneo and the mountainous region in Papua. The CDD, on the other hand, has a significant positive trend over southern Sumatra and in Java. Moreover, the increase of CDD in Indonesia is higher than in other regions in SEA. This indicates that a condition toward dryer conditions is higher in the Indonesia region than in other regions in the SEA.

4.2 Extreme hydrological changes

Investigating climate change's impact on global streamflow, Van Vliet et al. (2013) discovered an indication of changes in seasonal flow amplitudes, magnitude, and timing of high and low flow events. They projected that the mean flow and low flow will decline over SEA in the future. This is supported by other previous studies showing the streamflow change over the Johor (Tan et al., 2019) and Kelantan (Tan et al., 2020) river basins in Malaysia. In addition, they projected that the meteorological drought is likely to become longer at the end of the 21st century. However, it is still not clear whether the hydrological drought will have a longer duration. Although results from a study on meteorological drought - focusing on short-term precipitation



shortage - not necessarily coincides with hydrological drought, low flow most likely will occur during an extreme drought event (Sutanto and Van Lanen, 2021). Similar to the global study conducted by Van Vliet et al. (2013), our research is in agreement with their finding concluded that over SEA, the impact of extreme climate change in the near future is more prominent for the low flow than high flow conditions, especially in Indonesia.

355 The impact of changes in climate indices in SEA also affects the changes in hydrological extremes. The increase of CDD over Northern MEB (northern 24°N) results in declining LFD over the central part of MEB, especially over northern Laos. Our results also show that the increase of Rx1day and R95pTOT over the northern MEB does not significantly trigger the HFD over the northern and central parts of MEB. However, the increase of Rx1day, R95pTOT, and SDII over the southern MEB yields higher HFD and the probability of high flow events over Thailand and Cambodia.

360 In the southern part of Sumatra and in the centre of the Malaysian peninsula, the CDD will increase in the near future, reducing the LFD across the region. This might be caused by the increase of CDD5D that spreads more than CDD. The increase of SDII over the Southern part of Sumatra and the eastern part of the Malaysian peninsula results in higher streamflow and the probability of HFD in some rivers in these regions.

The increasing CDD that spreads in the majority of areas of Java makes most rivers on the island show a decrease in LFD.
365 Increasing Rx1day, R95pTOT, and SDII over the north coast of the western part of the island lead to higher HFD and an increase in the probability of high flow events.

In Borneo, the increase of CDD in the Southern part and CDD5D in most areas of the island decrease the LFD and increase the probability of low flow events. Although the increasing Rx1day is visible only in some areas in Borneo, most areas show higher R95pTOT and SDII. As a result, most of the rivers in Borneo have higher HFD and probability of high flow events.

370 Multiple sectors can be affected by the change of LFD. The likely impact of decreasing LFD over SEA will pose a challenge to some sectors such as agriculture, hydropower, industry, and public water supply. Mentioned by Horton et al. (2022), the decreasing flow in the early wet season in the future over the Cambodian Mekong floodplain will affect rice production. In addition, in Laos, hydropower will face challenges due to a 22% decrease in LFD and an 85% increase of probability low flow events in the central part of MEB. Meanwhile, over Sumatra, two big hydropowered rivers will also face issues with decreasing
375 LDF. The two hydropower sectors are firstly the Sigura-Gura hydropower located in the north part of Sumatra that will face a 15% LFD decrease and an 88% increasing probability of low flow events of the Asahan River. Secondly, in the western part, the Musi Bengkulu hydropower will face a 23% LFD decrease and a 75% increasing probability of low flow events of the Musi River. On another Island of Indonesia, Java, the Mrica hydropower on the Serayu river in the central part of the island will face a 17% LFD decrease and a 68% increasing probability of a low flow event. Over Borneo, the Kayan River will face an 8%
380 LFD decrease and an 80% increasing probability of low flow events, this condition needs to be considered for the planning of the Kayan hydropower project which will be one of the biggest hydropower plants in SEA and will provide electricity for the new capital of Indonesia (Ibu Kota Nusantara - IKN). The increase in extreme dry rainfall conditions will decrease the LFD resulting in low water table in the soil. In Borneo, these conditions will decrease the peatland's water table, which will increase the risk of forest fires in that area and, for similar reasons, over Sumatra island (Taufik et al., 2017).



385 4.3 Impact of catchment properties on hydrological extremes

The impact of climate change varies between rivers depending on the catchment characteristics. This also applies to extreme events, such as floods, drought, high flow, and low flow as shown in our study. Previous studies on drought demonstrated that hydrological extremes are not only influenced by climate but also by the catchment properties (Van Lanen et al., 2013; Van Loon and Laaha, 2015; Sutanto and Van Lanen, 2022). In our study, the role of the physical characteristics of the river can be clearly seen in the low flow analysis. To investigate the impact of catchment characteristics on the low flow, we calculated the river recession constant (C) (Gustard and Demuth, 2009). The C value shows the overall recession rate in days, in which the small (high) C indicates a flashy (gentle) hydrograph of the river (Gustard and Demuth, 2009). One should note that the recession constant (C) is not the same as the recession coefficient (RC). A flashy hydrograph indicates that the river has a high risk of a flash flood, while a gentle hydrograph has a low risk of a flash flood. A description of how to calculate C and the plots over four selected domains are available in supplementary material 8.

In MEB, increasing CDD over the northern part of the region has more impact on LFD over the central part of the basin. A similar result was also found in Java, where increasing CDD across the island has more impact on LFD for rivers flowing in the western part of the island. The C analysis shows that these rivers have relatively small C . We found that rivers with small C (flashy hydrograph) are more susceptible to LFD changes than rivers with high C (gentle hydrograph), associated with catchment properties. Some interesting results are also found over Sumatra and Java regarding increasing the probability of low flow events. Although it did not show a relatively high decreasing LFD than other rivers in each domain, rivers in the Northern part of Sumatra, the Eastern part of Java, the southern part of Borneo, and also the eastern part of Borneo show a significant increase in the probability of low flow events. Those rivers are found to have a relatively high C value.

Next, We discuss the relation between the change in low flow and catchment properties denoted by C by plotting the density of the streamflow over three rivers for historical and near future periods. The plot of the density of the discharge over three rivers is available in supplement material 9. The Bengawan Solo river located in the eastern part of Java and the Kampar river located in the northern part of Sumatra are rivers that have high C values. We compared those rivers with the Batanghari river which is situated in the southern part of Sumatra that has a small C value. Here we found that rivers with high C values have a more narrow streamflow distribution than rivers with small C values. This is due to the more steady and less flashy streamflow characteristic of high C value rivers. As a result, the shift of streamflow distribution for high C value rivers triggers a higher probability of low flow change than for small C value rivers.

4.4 Sources of uncertainty

In this study, we used one climate scenario; RCP 8.5 which the projection is simulated based on a high future emissions scenario for temperature and greenhouse gasses (global warming scenario). This scenario becomes one of the sources of uncertainty in projections. Lehner et al. (2020) reported that major uncertainty for the near future (until 2050) rainfall projection comes from the model spread instead of the RCP scenario spread. The consideration of applying only one scenario in this analysis is due to the relatively small differences between RCP scenarios in the near future climate projection (IPCC, 2021). Moreover, the



RCP8.5 scenario has covered the extreme spectrum of climate projection. The model spread has the biggest impact on the near future rainfall projection. In this study, in order to reduce the uncertainty coming from this source, we employ 5 high-resolution GCMs (10 members in total).

Another source of uncertainty comes from the hydrological model. In this study, we applied only one hydrological model (PCR-GLOBWB), which is a limitation of this study. This study, however, focuses on the impacts of extreme climates on future high and low flows. The PCR-GLOBWB model is one of the global hydrological models that run in high resolution globally and it is proven to be reliable for extreme studies (Trambauer et al., 2014; Ward et al., 2013). In this study, the hydrological model simulation does not consider water demand. This also can be one of the uncertainties of the near future flow analysis. The purpose of this setting is that we want to focus only on climate exposure on extreme streamflows. The uncertainty of the climate projections is propagated through the hydrological model by forcing the hydrological model with each available member of the climate model ensemble.

5 Conclusions

The SEA region will experience an increase in both dry and wet extremes in near future. Myanmar and the Malaysian peninsula will face more challenges due to climate change compared to other areas in the Indochina region as the changes are the strongest in these regions. The northern part of Myanmar will experience an increase in dry spell length (CDD), while the west coast of Myanmar will experience more extreme rainfall (in terms of the wettest day of the year, Rx1day, the wettest 5-day spell of the year, Rx5day, and the number of very wet days, R95pTOT). The Malaysian Peninsula will also experience increasingly long dry spells (CDD, CDD5D), wet spells with excessive amounts of rain (Rx5day50mm) and an increase in the intensity of rainfall (SDII). The amount of rainfall due to very wet days in Malaysia (R95pTOT) will increase in the near future. Furthermore, increasing dry spell length (CDD) is also found in the Central part of the Philippines, along with an increase in rainfall intensity in the northern Philippines. Over the Indonesian Maritime continents, Sumatra and Borneo will experience more extreme conditions of dry and wet events in the near future. The southern part of Sumatra and Java will be affected by the highest increase of dry spell length (CDD) up to 40% in the SEA. In addition, Sumatra, Borneo, and Papua will experience increasingly intense rainfall (SDII) and stronger rainfall extremes (R10mm, R20mm, Rx1day, R95pTOT).

As a result of changing rainfall, we found decreasing and increasing low flow (LFD) and high flow (HFD), respectively along with the increasing probability of low flow and high flow events in the near future. A drier condition during the low flow event is more prominent compared to the wet condition during the high flow event. In the Mekong basin, the decrease in streamflow and increase in the probability of low flow events are found in the Central and Southern parts of the Basin, with higher change in the central part. In contrast, increasing discharge and probability of high flow events are projected in the southern part of the basin, especially in Thailand and Cambodia. Drier conditions during the low flow event and the increase in the probability of low flow events were simulated in most of the rivers located in the Malaysian peninsula, Sumatra, Borneo, and Java. The increase of high flow and its probability is found in some rivers situated in the Malaysian peninsula, western Java, and the



450 majority of rivers in Borneo. In general, rivers in Borneo will experience more severe conditions during both low flow and high flow events.

Our study also concluded that rivers in Sumatra and Java that have a less steady and more variable or ‘flashy’ streamflow (quantified as steep-slope hydrographs) are likely to experience more decreasing low flow in the future than rivers with a shallow-slope hydrograph. However, these latter rivers will have a greater risk of increasing the probability of low flow events
455 than the rivers with steep-slope hydrographs. This is associated with the characteristic of shallow-slope rivers that generates a narrow discharge distribution. Our study reveals that the changes in low flow events and their probabilities are not only influenced by extreme dry climates but also by the catchment characteristics.

Code availability. PCR-GLOBWB model is available in https://github.com/UU-Hydro/PCR-GLOBWB_model

Data availability. The climate model output from the high-resolution model intercomparison project (HighResMIP) is available from the
460 H2020-funded Primavera project (<https://www.primavera-h2020.eu/>) and the APHRODITE grided precipitation and temperature datasets are available in <http://aphrodite.st.hirosaki-u.ac.jp/products.html>

Author contributions. Gerard van der Schrier: Conceptualization; resources; supervision; review. Gert-Jan Steeneveld: Supervision; review. Samuel J. Sutanto: Conceptualization; supervision; review. Edwin Sutanudjaja: Software. Dian Nur Ratri: Writing and editing. Ardhasena Sopaheluwakan: Supervision. Albert Klein Tank: Supervision; project administration.

465 *Competing interests.* The authors declare that they have no known competing interests or personal relationships that could have appeared to influence the work reported in this paper.

Acknowledgements. The First author received funding from the Indonesia Endowment Fund for Education (LPDP)(S-353/LPDP.3/2019) for his PhD program. The second author acknowledges the support of the Royal Netherlands Embassy in Jakarta, Indonesia, through a Joint Cooperation Programme between Dutch and Indonesian research institutes. The HighResMIP simulations have been made available through
470 the PRIMAVERA project which received funding from the European Union’s Horizon 2020 Research and Innovation Programme under grant agreement no. 641727. This PRIMAVERA data is part of the IS-ENES3 project that has received funding from the European Union’s Horizon 2020 research and innovation programme under grant agreement No. 824084.



References

- Aldrian, E. and Susanto, D.: Identification of three dominant rainfall regions within Indonesia and their relationship to sea surface temperature, *Int. J. Clim.*, 23, 1435–1454, doi : 10.1002/joc.950, 2003.
- Ali, H. and Mishra, V.: Contrasting response of rainfall extremes to increase in surface air and dewpoint temperatures at urban locations in India, *Scientific reports*, 7, 1–15, doi : 10.1038/s41598-017-01306-1, 2017.
- Amengual, A., Homar, V., Romero, R., Alonso, S., and Ramis, C.: A statistical adjustment of regional climate model outputs to local scales: application to Platja de Palma, Spain, *Journal of Climate*, 25, 939–957, doi : 10.1175/JCLI-D-10-05024.1, 2012.
- 475 Amsal, F., Harsa, H., Sopaheluwakan, A., Linarka, U., Pradana, R., and Satyaningsih, R.: Bias correction of daily precipitation from down-scaled CMIP5 climate projections over the Indonesian region, in: *IOP Conf. Ser.: Earth Environ. Sci.*, vol. 303, p. 012046, IOP Publishing, doi : 10.1088/1755-1315/303/1/012046, 2019.
- Asadieh, B. and Krakauer, N. Y.: *Global change in streamflow extremes under climate change over the 21st century*, *Hydrol. Earth Syst. Sci.*, 21, 5863–5874, doi : 10.5194/hess-21-5863-2017, 2017.
- 485 Benestad, R. E., Lussana, C., Lutz, J., Dobler, A., Landgren, O., Haugen, J. E., Mezghani, A., Casati, B., and Parding, K. M.: *Global hydro-climatological indicators and changes in the global hydrological cycle and rainfall patterns*, *PLOS Climate*, 1, e0000029, doi=10.1371/journal.pclm.0000029, 2022.
- Bierkens, M. and Van Beek, L.: *Seasonal predictability of European discharge: NAO and hydrological response time*, *Journal of Hydrometeorology*, 10, 953–968, doi : 10.1175/2009JHM1034.1, 2009.
- 490 Block, P. J., Souza Filho, F. A., Sun, L., and Kwon, H.-H.: *A streamflow forecasting framework using multiple climate and hydrological models 1*, *JAWRA Journal of the American Water Resources Association*, 45, 828–843, 2009.
- Boé, J., Terray, L., Habets, F., and Martin, E.: *Statistical and dynamical downscaling of the Seine basin climate for hydro-meteorological studies*, *International Journal of Climatology: A Journal of the Royal Meteorological Society*, 27, 1643–1655, 2007.
- Cherchi, A., Fogli, P. G., Lovato, T., Peano, D., Iovino, D., Gualdi, S., Masina, S., Scoccimarro, E., Materia, S., Bellucci, A., and Navarra, A.: *Global mean climate and main patterns of variability in the CMCC-CM2 coupled model*, *J. Adv. Model. Earth Sy.*, 11, 185–209, doi : 10.1029/2018MS001369, 2019.
- 495 Cinco, T. A., de Guzman, R. G., Hilario, F. D., and Wilson, D. M.: *Long-term trends and extremes in observed daily precipitation and near surface air temperature in the Philippines for the period 1951–2010*, *Atmospheric Research*, 145, 12–26, 2014.
- Corporal-Lodangco, I. L. and Leslie, L. M.: *Climatology of Philippine tropical cyclone activity: 1945–2011*, *International Journal of Climatology*, 37, 3525–3539, 2017.
- 500 Cruz, F., Narisma, G., Dado, J., Singhruck, P., Tangang, F., Linarka, U., Wati, T., Juneng, L., Phan-Van, T., Ngo-Duc, T., et al.: *Sensitivity of temperature to physical parameterization schemes of RegCM4 over the CORDEX-Southeast Asia region*, *Int. J. Climatol.*, 37, 5139–5153, doi : 10.1002/joc.5151, 2017.
- Déqué, M., Rowell, D. P., Lüthi, D., Giorgi, F., Christensen, J., Rockel, B., Jacob, D., Kjellström, E., De Castro, M., and van den Hurk, B.: *An intercomparison of regional climate simulations for Europe: assessing uncertainties in model projections*, *Climatic Change*, 81, 53–70, 2007.
- 505 Ehret, U., Zehe, E., Wulfmeyer, V., Warrach-Sagi, K., and Liebert, J.: *HESS opinions: “Should we apply bias correction to global and regional climate model data?”*, *Hydrol. Earth Syst. Sci.*, 16, 3391–3404, 2012.



- 510 Fang, G., Yang, J., Chen, Y., and Zammit, C.: Comparing bias correction methods in downscaling meteorological variables for a hydrologic impact study in an arid area in China, *Hydrology and Earth System Sciences*, 19, 2547–2559, 2015.
- Funk, C., Peterson, P., Landsfeld, M., Pedreros, D., Verdin, J., Shukla, S., Husak, G., Rowland, J., Harrison, L., Hoell, A., et al.: The climate hazards infrared precipitation with stations—a new environmental record for monitoring extremes, *Scientific Data*, 2, 150066, doi : 10.1038/sdata.2015.66, 2015.
- 515 Gupta, H. V., Kling, H., Yilmaz, K. K., and Martinez, G. F.: Decomposition of the mean squared error and NSE performance criteria: Implications for improving hydrological modelling, *Journal of hydrology*, 377, 80–91, 2009.
- Gustard, A. and Demuth, S.: *Manual on low-flow estimation and prediction. Operational hydrology report, No. 50 WMO-No. 1029*, World Meteorological Organization, Geneva, Switzerland, 136, 2009.
- 520 Haarsma, R., Acosta, M., Bakhshi, R., Bretonnière, P.-A. B., Caron, L.-P., Castrillo, M., Corti, S., Davini, P., Exarchou, E., Fabiano, F., Fladrich, U., Fuentes Franco, R., García-Serrano, J., von Hardenberg, J., Koenigk, T., Levine, X., Meccia, V., van Noije, T., van den Oord, G., Palmeiro, F. M., Rodrigo, M., Ruprich-Robert, Y., Le Sager, P., Tourigny, E., Wang, S., van Weele, M., and Wyser, K.: HighResMIP versions of EC-Earth: EC-Earth3P and EC-Earth3P-HR. Description, model performance, data handling and validation, *Geosci. Model Dev. Discussions*, 2020, 1–37, <https://www.geosci-model-dev-discuss.net/gmd-2019-350/>, doi : 10.5194/gmd-2019-350, 2020.
- 525 Haarsma, R. J., Roberts, M. J., Vidale, P. L., Senior, C. A., Bellucci, A., Bao, Q., Chang, P., Corti, S., Fučkar, N. S., Guemas, V., von Hardenberg, J., Hazeleger, W., Kodama, C., Koenigk, T., Leung, L. R., Lu, J., Luo, J. J., Mao, J., Mizielinski, M. S., Mizuta, R., Nobre, P., Satoh, M., Scoccimarro, E., Semmler, T., Small, J., and von Storch, J. S.: High Resolution Model Intercomparison Project (HighResMIP v1. 0) for CMIP6, *Geoscientific Model Development*, 9, 4185–4208, doi : 10.5194/gmd-9-4185-2016, 2016.
- Hamada, J.-I., D Yamanaka, M., Matsumoto, J., Fukao, S., Winarso, P. A., and Sribimawati, T.: Spatial and temporal variations of the rainy season over Indonesia and their link to ENSO, *Journal of the Meteorological Society of Japan. Ser. II*, 80, 285–310, doi : 10.2151/jmsj.80.285, 2002.
- 530 Hamon, W. R.: Estimating potential evapotranspiration, *Journal of the Hydraulics Division*, 87, 107–120, 1961.
- Hariadi, M., van der Schrier, G., Steeneveld, G.-J., Ratri, D., Sopaheluwakan, A., Tank, A., Aldrian, E., Gunawan, D., Moine, M.-P., Bellucci, A., Senan, R., Tourigny, E., Putrasahan, D., and Linarko, A.: Evaluation of extreme precipitation over Southeast Asia in the CMIP5 regional climate model results and HighResMIP global climate models, *International Journal of Climatology*, 2022.
- 535 Hariadi, M. H.: *Projected drought severity changes in Southeast Asia under medium and extreme climate change*, Ph.D. thesis, Wageningen University and Research, 2017.
- Hariadi, M. H., van der Schrier, G., Steeneveld, G. J., Sopaheluwakan, A., Klein Tank, A. M. G., Roberts, M. J., Moine, M. P., Bellucci, A., Senan, R., Tourigny, E., and Putrasahan, D.: Evaluation of onset, cessation and seasonal precipitation of the Southeast Asia rainy season in CMIP5 regional climate models and HighResMIP global climate models, *International Journal of Climatology*, doi : 10.1002/joc.7404, 2021.
- 540 Hijioka, Y., Lin, E., Pereira, J. J., Corlett, R., Cui, X., Inсарov, G., Lasco, R., Lindgren, E., and Surjan, A.: Asia. Climate change 2014: impacts, adaptation, and vulnerability. Part B: regional aspects. Contribution of working group II to the fifth assessment report of the intergovernmental panel on climate change(pp. 1327–1370), Cambridge university press, Cambridge, United Kingdom and New York, NY, USA, 2014.
- 545 Hisdal, H., Tallaksen, L. M., Clausen, B., Peters, E., and Gustard, A.: A Hydrological Drought Characteristics. In: Tallaksen, L. M. & Van Lanen, H. A. J. (Eds.) *Hydrological Drought, Processes and Estimation Methods for Streamflow and Groundwater*, vol. Development in Water Science 48, Elsevier Science B.V., 2004.



- Hoang, L. P., Lauri, H., Kumm, M., Koponen, J., Van Vliet, M. T., Supit, I., Leemans, R., Kabat, P., and Ludwig, F.: Mekong river flow and hydrological extremes under climate change, *Hydrology and Earth System Sciences*, 20, 3027–3041, 2016.
- Horton, A. J., Triet, N. V., Hoang, L. P., Heng, S., Hok, P., Chung, S., Koponen, J., and Kumm, M.: The Cambodian Mekong floodplain under future development plans and climate change, *Natural Hazards and Earth System Sciences*, 22, 967–983, 2022.
- Huang, S., Huang, Q., Chang, J., and Leng, G.: Linkages between hydrological drought, climate indices and human activities: a case study in the Columbia river basin, *International Journal of climatology*, 36, 280–290, 2016.
- IPCC: *Climate Change 2021: the Physical Science Basis*. [Masson-Delmotte, V., P. Zhai, A. Pirani, S.L. Connors, C. Péan, S. Berger, N. Caud, Y. Chen, L. Goldfarb, M.I. Gomis, M. Huang, K. Leitzell, E. Lonnoy, J.B.R. Matthews, T.K. Maycock, T. Waterfield, O. Yelekçi, R. Yu, and B. Zhou (eds.)], *Contribution of Working Group I to the Sixth Assessment Report of the Intergovernmental Panel on Climate Change*, doi : 10.1017/9781009157896, 2021.
- Jasparro, C. and Taylor, J.: Climate change and regional vulnerability to transnational security threats in Southeast Asia, *Geopolitics*, 13, 232–256, 2008.
- Juneng, L., Tangang, F., Chung, J. X., Ngai, S. T., Tay, T. W., Narisma, G., Cruz, F., Phan-Van, T., Ngo-Duc, T., Santisirisomboon, J., Singhruck, P., Gunawan, D., and Aldrian, E.: Sensitivity of Southeast Asia rainfall simulations to cumulus and air-sea flux parameterizations in RegCM4, *Climate Research*, 69, 59–77, doi : 10.3354/cr01386, 2016.
- Klein Tank, A. M. G., Zwiers, F. W., and Zhang, X.: *Guidelines on analysis of extremes in a changing climate in support of informed decisions for adaptation*, World Meteorological Organization, wCDMP-No 72. WMO-TD No 1500:56, 2009.
- Knox, J., Hess, T., Daccache, A., and Wheeler, T.: Climate change impacts on crop productivity in Africa and South Asia, *Environmental research letters*, 7, 034 032, 2012.
- Lehner, F., Deser, C., Maher, N., Marotzke, J., Fischer, E. M., Brunner, L., Knutti, R., and Hawkins, E.: Partitioning climate projection uncertainty with multiple large ensembles and CMIP5/6, *Earth System Dynamics*, 11, 491–508, doi : 10.5194/esd-11-491-2020, 2020.
- Li, Z., Yu, W., Li, T., Murty, V., and Tangang, F.: Bimodal character of cyclone climatology in the Bay of Bengal modulated by monsoon seasonal cycle, *Journal of Climate*, 26, 1033–1046, doi :10.1175/JCLI-D-11-00627.1, 2013.
- Limsakul, A., Limjirakan, S., and Sriburi, T.: Observed changes in daily rainfall extreme along Thailand’s Coastal Zones, *Applied Environmental Research*, 32, 49–68, 2010.
- Lin, H.-I., Yu, Y.-Y., Wen, F.-I., and Liu, P.-T.: Status of Food Security in East and Southeast Asia and Challenges of Climate Change, *Climate*, 10, 40, 2022.
- Lobligeois, F., Andréassian, V., Perrin, C., Tabary, P., and Loumagne, C.: When does higher spatial resolution rainfall information improve streamflow simulation? An evaluation using 3620 flood events, *Hydrology and Earth System Sciences*, 18, 575–594, 2014.
- Luu, L. N., Scussolini, P., Kew, S., Philip, S., Hariadi, M. H., Vautard, R., Mai, K. V., Vu, T. V., Truong, K. B., Otto, F., van der Schrier, G., van Aalst, M. K., and van Oldenborgh, G. J.: Attribution of typhoons-induced torrential precipitation in Central Vietnam, October 2020, *Climatic Change*, 2021.
- Mair, A. and Fares, A.: Influence of groundwater pumping and rainfall spatio-temporal variation on streamflow, *Journal of Hydrology*, 393, 287–308, <https://doi.org/https://doi.org/10.1016/j.jhydrol.2010.08.026>, 2010.
- Mehran, A., AghaKouchak, A., and Phillips, T. J.: Evaluation of CMIP5 continental precipitation simulations relative to satellite-based gauge-adjusted observations, *Journal of Geophysical Research: Atmospheres*, 119, 1695–1707, 2014.
- Moron, V., Robertson, A. W., and Boer, R.: Spatial coherence and seasonal predictability of monsoon onset over Indonesia, *J. Climate*, 22, 840–850, doi : 10.1175/2008JCLI2435.1, 2009.



- 585 Müller, W. A., Jungclaus, J. H., Mauritsen, T., Baehr, J., Bittner, M., Budich, R., Bunzel, F., Esch, M., Ghosh, R., Haak, H., Ilmarinen, T., Kleine, T., Kornblüeh, L., Li, H., Modali, K., Notz, D., Pohlmann, H., Roeckner, E., Stemmler, I., Tian, F., and Marotzke, J.: A Higher-resolution Version of the Max Planck Institute Earth System Model (MPI-ESM1.2-HR), *J. Adv. Model. Earth Sy.*, 10, 1383–1413, 2018.
- Ngai, S. T., Tangang, F., and Juneng, L.: Bias correction of global and regional simulated daily precipitation and surface mean temperature over Southeast Asia using quantile mapping method, *Global and Planetary Change*, 149, 79–90, 2017.
- 590 Ngai, S. T., Juneng, L., Tangang, F., Chung, J. X., Salimun, E., Tan, M. L., and Amalia, S.: Future projections of Malaysia daily precipitation characteristics using bias correction technique, *Atmospheric Research*, 240, 104 926, 2020a.
- Ngai, S. T., Sasaki, H., Murata, A., Nosaka, M., Chung, J. X., Juneng, L., Salimun, E., Tangang, F., et al.: Extreme rainfall projections for Malaysia at the end of 21st century using the high resolution non-hydrostatic regional climate model (NHRCM), *SOLA*, 2020b.
- Ngo-Duc, T., Tangang, F. T., Santisirisonboon, J., Cruz, F., Trinh-Tuan, L., Nguyen-Xuan, T., Phan-Van, T., Juneng, L., Narisma, G., Singhruck, P., Gunawan, D., and Aldrian, E.: Performance evaluation of RegCM4 in simulating extreme rainfall and temperature indices over the CORDEX-Southeast Asia region, *Int. J. Climatol.*, 37, 1634–1647, doi : 10.1002/joc.4803, 2017.
- 595 Nguyen-Ngoc-Bich, P., Phan-Van, T., Ngo-Duc, T., Vu-Minh, T., Trinh-Tuan, L., Tangang, F. T., Juneng, L., Cruz, F., Santisirisonboon, J., Narisma, G., et al.: Projected evolution of drought characteristics in Vietnam based on CORDEX-SEA downscaled CMIP5 data, *International Journal of Climatology*, 41, 5733–5751, 2021.
- 600 Nguyen-Thi, H. A., Matsumoto, J., Ngo-Duc, T., and Endo, N.: A climatological study of tropical cyclone rainfall in Vietnam, *Sola*, 8, 41–44, 2012.
- Piani, C., Weedon, G., Best, M., Gomes, S., Viterbo, P., Hagemann, S., and Haerter, J.: Statistical bias correction of global simulated daily precipitation and temperature for the application of hydrological models, *Journal of hydrology*, 395, 199–215, 2010.
- Ratri, D. N., Whan, K., and Schmeits, M.: A comparative verification of raw and bias-corrected ECMWF seasonal ensemble precipitation reforecasts in Java (Indonesia), *Journal of Applied Meteorology and Climatology*, 58, 1709–1723, 2019.
- 605 Redfern, S. K., Azzu, N., Binamira, J. S., et al.: Rice in Southeast Asia: facing risks and vulnerabilities to respond to climate change, *Build Resilience Adapt Climate Change Agri Sector*, 23, 1–14, 2012.
- Renard, B. and Thyer, M.: Revealing hidden climate indices from the occurrence of hydrologic extremes, *Water Resources Research*, 55, 7662–7681, 2019.
- 610 Roberts, M. J., Baker, A., Blockley, E. W., Calvert, D., Coward, A., Hewitt, H. T., Jackson, L. C., Kuhlbrodt, T., Mathiot, P., Roberts, C. D., Schiemann, R., Seddon, J., Vannièrè, B., and Vidale, P. L.: Description of the resolution hierarchy of the global coupled HadGEM3-GC3.1 model as used in CMIP6 HighResMIP experiments, *Geosci. Model Dev.*, 12, 4999–5028, doi : 10.5194/gmd-12-4999-2019, 2019.
- Roberts, M. J., Camp, J., Seddon, J., Vidale, P. L., Hodges, K., Vannièrè, B., Mecking, J., Haarsma, R., Bellucci, A., Scoccimarro, E., Caron, L. P., Chauvin, F., Terray, L., Valcke, S., Moine, M. P., Putrasahan, D., Roberts, C. D., Senan, R ana Zarzycki, C., Ullrich, P., Yamada, Y., Mizuta, R., Kodama, C., Fu, D., Zhang, Q., Danabasoglu, G., Rosenbloom, N., Wang, H., and Wu, L.: Projected future changes in tropical cyclones using the CMIP6 HighResMIP multimodel ensemble, *Geophysical Research Letters*, 47, e2020GL088 662, 2020.
- 615 Ruijsch, J., Verstegen, J. A., Sutanudjaja, E. H., and Karssenber, D.: Systemic change in the Rhine-Meuse basin: Quantifying and explaining parameters trends in the PCR-GLOBWB global hydrological model, *Advances in Water Resources*, 155, 104 013, 2021.
- Schulzweida, U. and Quast, R.: Climate indices with CDO, url : earth.bsc.es/gitlab/ces/cdo/raw/b4f0edf2d5c87630ed4c5ddee5a4992e3e08b06a/doc/cdo_...
- 620 2015.
- Schulzweida, U., Kornblüeh, L., and Quast, R.: CDO user's guide, *Climate Data Operators, Version, 1*, 205–209, 2006.



- Sen, P. K.: Estimates of the regression coefficient based on Kendall's tau, *Journal of the American statistical association*, 63, 1379–1389, 1968.
- Singh, V. and Xiaosheng, Q.: Data assimilation for constructing long-term gridded daily rainfall time series over Southeast Asia, *Climate Dynamics*, 53, 3289–3313, 2019.
- 625 Siswanto, S., van Oldenborgh, G. J., van der Schrier, G., Jilderda, R., and van den Hurk, B.: Temperature, extreme precipitation, and diurnal rainfall changes in the urbanized Jakarta city during the past 130 years, *International Journal of Climatology*, 36, 3207–3225, doi : 10.1002/joc.4548, 2016.
- Smit, B. and Wandel, J.: Adaptation, adaptive capacity and vulnerability, *Global Environmental Change*, 16, 282–292, <https://doi.org/https://doi.org/10.1016/j.gloenvcha.2006.03.008>, resilience, Vulnerability, and Adaptation: A Cross-Cutting Theme of the International Human Dimensions Programme on Global Environmental Change, 2006.
- 630 Sperna Weiland, F., Van Beek, L., Kwadijk, J., and Bierkens, M.: The ability of a GCM-forced hydrological model to reproduce global discharge variability, *Hydrology and Earth System Sciences*, 14, 1595–1621, 2010.
- Stahl, K., Kohn, I., Blauhut, V., Urquijo, J., De Stefano, L., Acacio, V., Dias, S., Stagge, J. H., Tallaksen, L. M., Kampragou, E., Van Loon, A. F., Barker, L. J., Melsen, L. A., Bifulco, C., Musolino, D., de Carli, A., Massarutto, A., Assimacopoulos, D., and Van Lanen, H. A. J.: Impacts of European drought events: insights from an international database of text-based reports, *Nat. Hazards Earth Syst. Sci.*, 16, 801–819, doi : 10.5194/nhess-16-801-2016, 2016.
- 635 Suhaila, J., Deni, S. M., Wan Zin, W. Z., and Jemain, A. A.: Spatial patterns and trends of daily rainfall regime in Peninsular Malaysia during the southwest and northeast monsoons: 1975–2004, *Meteorology and Atmospheric Physics*, 110, 1–18, 2010.
- 640 Supari, Tangang, F., Juneng, L., and Aldrian, E.: Observed changes in extreme temperature and precipitation over Indonesia, *International Journal of Climatology*, 37, 1979–1997, 2017.
- Supari, Tangang, F., Juneng, L., Faye, C., Jing Xiang, C., Sheau Tieh, N., Ester, S., Mohd, S. F. M., Jerasorn, S., Patama, S., Tan, P., Ngo-Duc, T., Gemma, N., Edvin, A., Dodo, G., and Ardhasena, S.: Multi-model projections of precipitation extremes in Southeast Asia based on CORDEX-Southeast Asia simulations, *Environmental Research*, 184, 109350, doi : 10.1016/j.envres.2020.109350, 2020.
- 645 Sutanto, S. J. and Van Lanen, H. A. J.: Streamflow drought: implication of drought definitions and its application for drought forecasting, *Hydrol. Earth Syst. Sci.*, 25, 3991–4023, doi : 10.5194/hess-25-3991-2021, 2021.
- Sutanto, S. J. and Van Lanen, H. A. J.: Catchment memory explains hydrological drought forecast performance, *Scientific Report*, 12, doi : 10.1038/s41598-022-06553-5, 2022.
- 650 Sutanudjaja, E. H., Van Beek, R., Wanders, N., Wada, Y., Bosmans, J. H., Drost, N., Van Der Ent, R. J., De Graaf, I. E., Hoch, J. M., De Jong, K., et al.: PCR-GLOBWB 2: a 5 arcmin global hydrological and water resources model, *Geoscientific Model Development*, 11, 2429–2453, 2018.
- Tallaksen, L. M., Madsen, H., and Clausen, B.: On the definition and modeling of streamflow drought duration and deficit volume, *Hydrological Sciences Journal*, 42, 15–33, doi : 10.1080/02626669709492003, 1997.
- Tan, M. L., Juneng, L., Tangang, F. T., Chan, N. W., and Ngai, S. T.: Future hydro-meteorological drought of the Johor river basin, Malaysia, based on CORDEX-SEA projections, *Hydrological Sciences Journal*, 64, 921–933, 2019.
- 655 Tan, M. L., Juneng, L., Tangang, F. T., Samat, N., Chan, N. W., Yusop, Z., and Ngai, S. T.: SouthEast Asia HydrO-meteorological drought (SEA-HOT) framework: A case study in the Kelantan river basin, Malaysia, *Atmospheric Research*, 246, 105155, 2020.
- Tangang, F., Supari, S., Chung, J. X., Cruz, F., Salimun, E., Ngai, S. T., Juneng, L., Santisirisomboon, J., Santisirisomboon, J., Ngo-Duc, T., Phan-Van, T., Narisma, G., Singhruck, P., Gunawan, D., Aldrian, E., Sopaheluwakan, A., Nikulin, G., Yang, H., Remedio, A. R. C., Sein,



- 660 D., and Hein-Griggs, D.: Future changes in annual precipitation extremes over Southeast Asia under global warming of 2 C, *APN Science Bulletin*, 8, 3–8, doi : 10.30852/sb.2018.436, 2018.
- Tangang, F., Santisirisomboon, J., Juneng, L., Salimun, E., Chung, J., Supari, S., Cruz, F., Ngai, S. T., Ngo-Duc, T., Singhruck, P., et al.: Projected future changes in mean precipitation over Thailand based on multi-model regional climate simulations of CORDEX Southeast Asia, *International Journal of Climatology*, 39, 5413–5436, 2019.
- 665 Taufik, M., Torfs, P. J., Uijlenhoet, R., Jones, P. D., Murdiyarso, D., and Van Lanen, H. A.: Amplification of wildfire area burnt by hydrological drought in the humid tropics, *Nature Climate Change*, 7, 428–431, 2017.
- Taylor, K. E., Stouffer, R. J., and Meehl, G. A.: An overview of CMIP5 and the experiment design, *Bulletin of the American meteorological Society*, 93, 485–498, 2012.
- Trambauer, P., Dutra, E., Maskey, S., Werner, M., Pappenberger, F., Van Beek, L., and Uhlenbrook, S.: Comparison of different evaporation
670 estimates over the African continent, *Hydrology and Earth System Sciences*, 18, 193–212, 2014.
- Trinh-Tuan, L., Matsumoto, J., Tangang, F. T., Juneng, L., Cruz, F., Narisma, G., Santisirisomboon, J., Phan-Van, T., Gunawan, D., Aldrian, E., and Ngo-Duc, T.: Application of quantile mapping bias correction for mid-future precipitation projections over Vietnam, *Sola*, 2019.
- Van Beek, L., Wada, Y., and Bierkens, M. F.: Global monthly water stress: 1. Water balance and water availability, *Water Resources Research*, 47, 2011.
- 675 van Beek, L. P., Eikelboom, T., van Vliet, M. T., and Bierkens, M. F.: A physically based model of global freshwater surface temperature, *Water Resources Research*, 48, 2012.
- Van den Besselaar, E. J., van der Schrier, G., Cornes, R. C., Iqbal, A. S., and Klein Tank, A. M.: SA-OBS: a daily gridded surface temperature and precipitation dataset for Southeast Asia, *J. Climate*, 30, 5151–5165, doi : 10.1175/JCLI-D-16-0575.1, 2017.
- Van Lanen, H. A. J., Wanders, N., Tallaksen, L. M., and Van Loon, A. F.: Hydrological drought across the world: impact of climate and
680 physical catchment structure, *Hydrol. Earth Syst. Sci.*, 17, 1715–1732, doi : 10.5194/hess-17-1715-2013, 2013.
- Van Loon, A. F. and Laaha, G.: Hydrological drought severity explained by climate and catchment characteristics, *Journal of Hydrology*, 526, 3–14, doi : 10.1016/j.jhydrol.2014.10.059, 2015.
- van Vliet, M. T., Franssen, W. H., Yearsley, J. R., Ludwig, F., Haddeland, I., Lettenmaier, D. P., and Kabat, P.: Global river discharge and water temperature under climate change, *Global Environmental Change*, 23, 459–464, doi : 10.1016/j.gloenvcha.2012.11.002, 2013.
- 685 Van Vliet, M. T., Ludwig, F., and Kabat, P.: Global streamflow and thermal habitats of freshwater fishes under climate change, *Climatic change*, 121, 739–754, 2013.
- Voldoire, A., Saint-Martin, D., Sénési, S., Decharme, B., Alias, A., Chevallier, M., Colin, J., Guérémy, J.-F., Michou, M., Moine, M.-P., et al.: Evaluation of CMIP6 DECK experiments with CNRM-CM6-1, *J. Adv. Model. Earth Sy.*, 11, 2177–2213, doi : 10.1029/2019MS001683, 2019.
- 690 Ward, P., Dettinger, M., Jongman, B., Kummerow, M., Sperna Weiland, F., and Winsemius, H.: Flood risk assessment at the global scale-the role of climate variability, in: *EGU General Assembly Conference Abstracts*, pp. EGU2013–1390, 2013.
- Weiss, J. et al.: *The economics of climate change in Southeast Asia: a regional review*, Asian Development Bank, 2009.
- Wong, W. K., Beldring, S., Engen-Skaugen, T., Haddeland, I., and Hisdal, H.: Climate Change Effects on Spatiotemporal Patterns of Hydro-climatological Summer Droughts in Norway, *J. Hydrometeorol.*, 12, 1205–1220, doi : 10.1175/2011JHM1357.1, 2011.
- 695 Yatagai, A., Kamiguchi, K., Arakawa, O., Hamada, A., Yasutomi, N., and Kitoh, A.: APHRODITE: constructing a long-term daily gridded precipitation dataset for Asia based on a dense network of rain gauges, *Bull. Am. Meteorol. Soc.*, 93, 1401–1415, doi : 10.1175/BAMS-D-11-00122.1, 2012.



Yevjevich, V.: An objective approach to definition and investigations of continental hydrologic droughts, Hydrology Papers 23, 1967.

Yusuf, A. A. and Francisco, H.: Climate change vulnerability mapping for Southeast Asia, 2009.

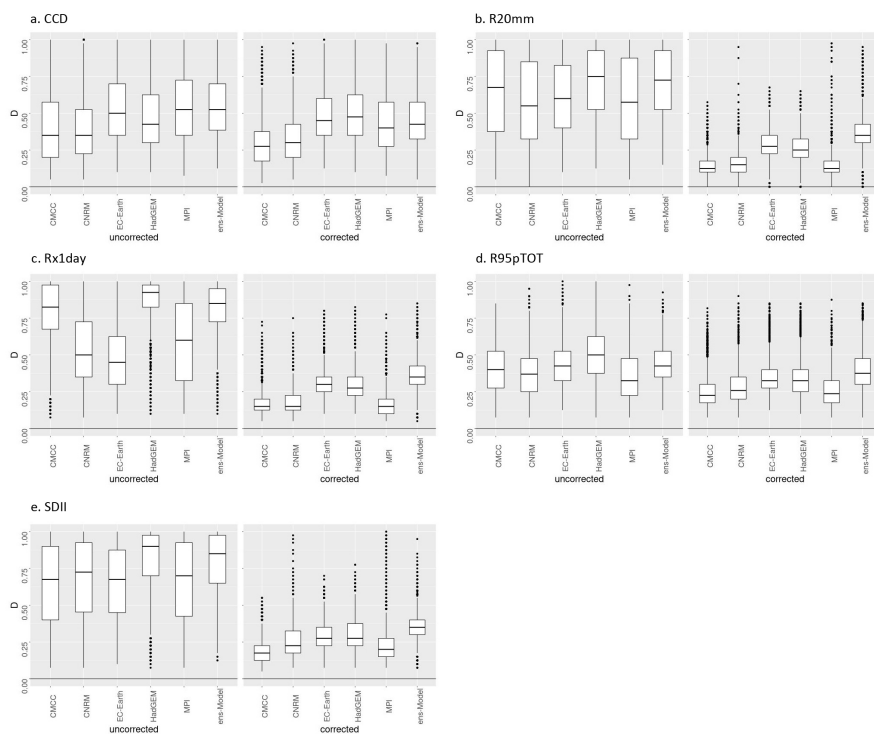


Figure 1. The Kolmogorov–Smirnov statistic value between the original model dataset and bias-corrected model dataset. The statistic value was calculated for simulating a) CDD, b) R20mm, c) Rx1day, d) R95pTOT and e) SDII.

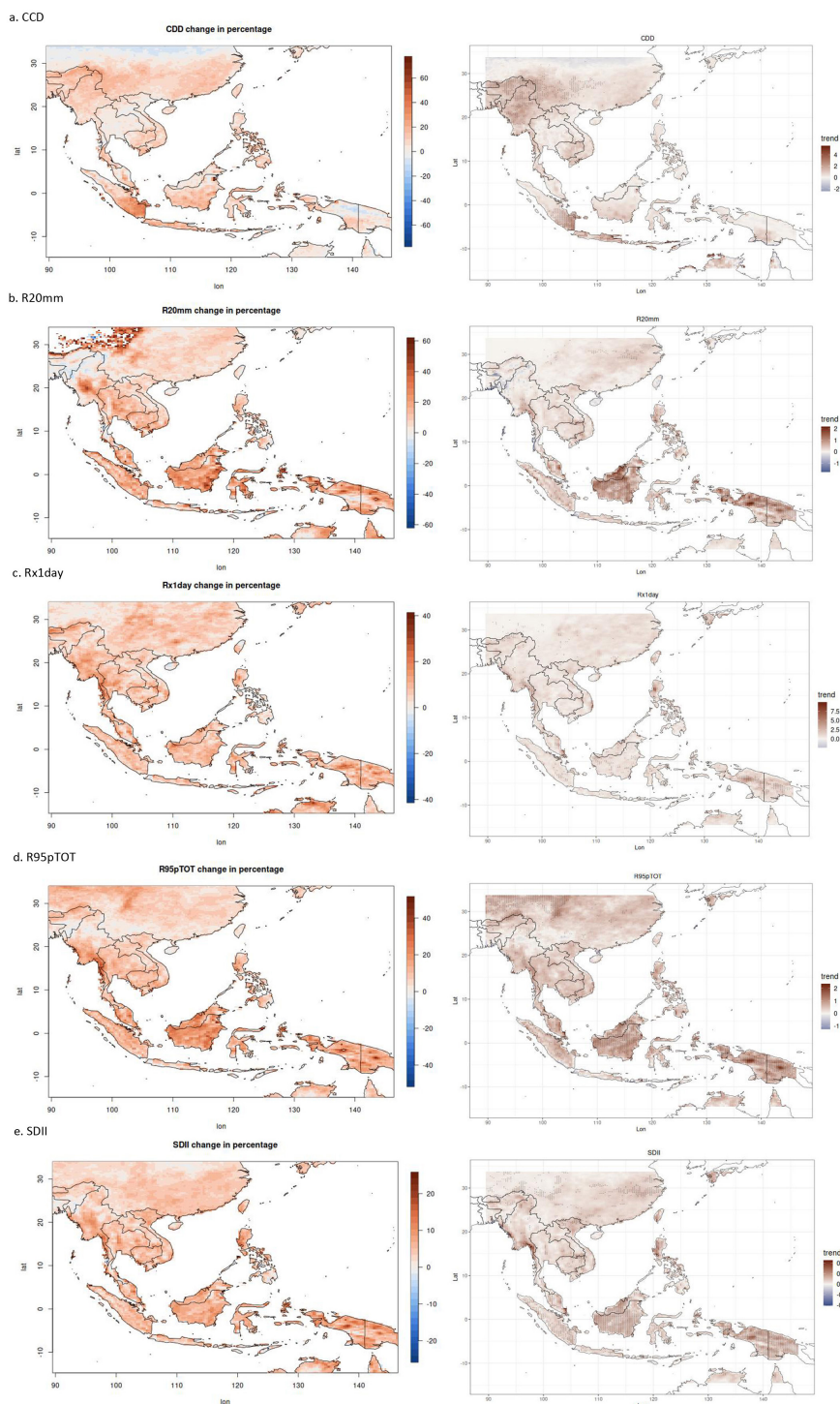


Figure 2. The change in percentage of the near future (2021-2050) compared to the historical period (1981-2010) (left), and the trend period 1971-2050 (right) for annually a) maximum length of a dry spell (CDD), b) a number of very heavy rainfall (R20mm), c) maximum daily rainfall (Rx1day), d) precipitation percent due to R95p days (R95pTOT) and e) simple daily intensity index (SDII). The dashes in the trend map indicate model agreement in the trend significant at 60% level agreement.

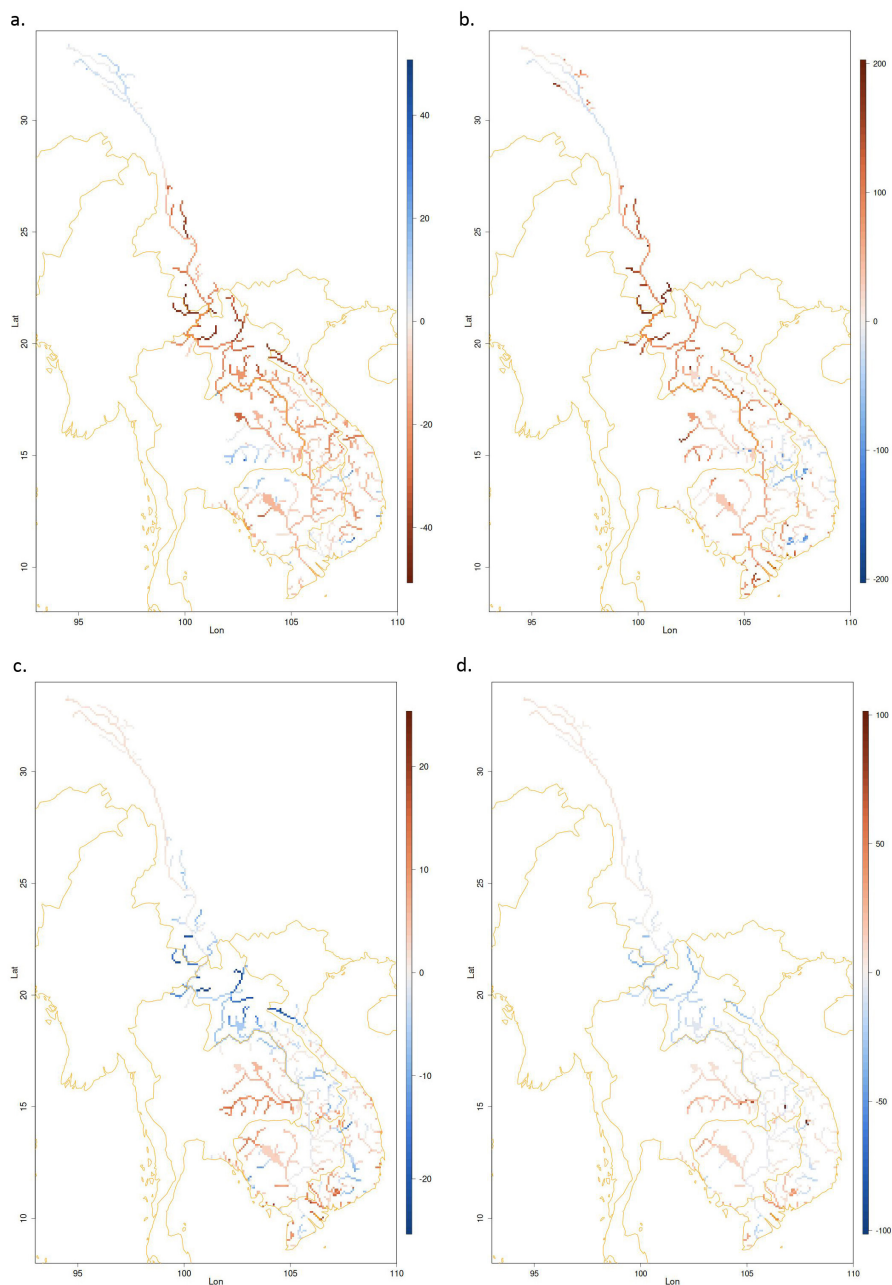


Figure 3. The change of extreme low (percentile 10) and extreme high (percentile 95) water discharge in the near future (2021-2050) compared to the historical period (1981-2010) over the Mekong region. Figure a: low flow magnitude change (%), figure b: low flow probability change (%), Figure c: high flow magnitude change (%) and figure d: high flow probability change (%)

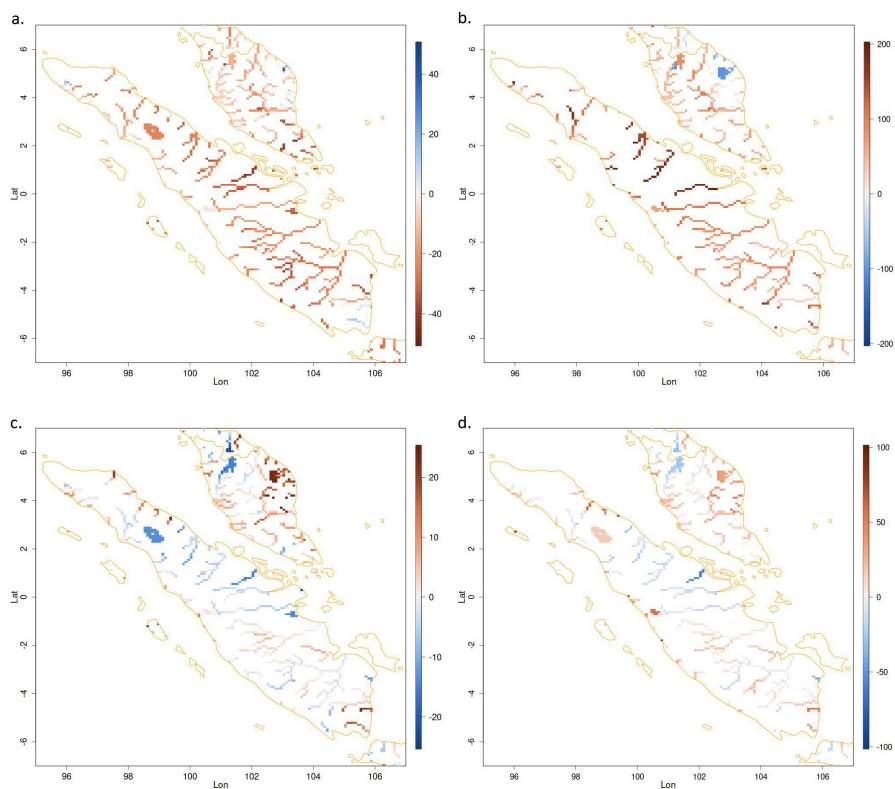


Figure 4. Similar to Fig. 3, but now for the Sumatra region

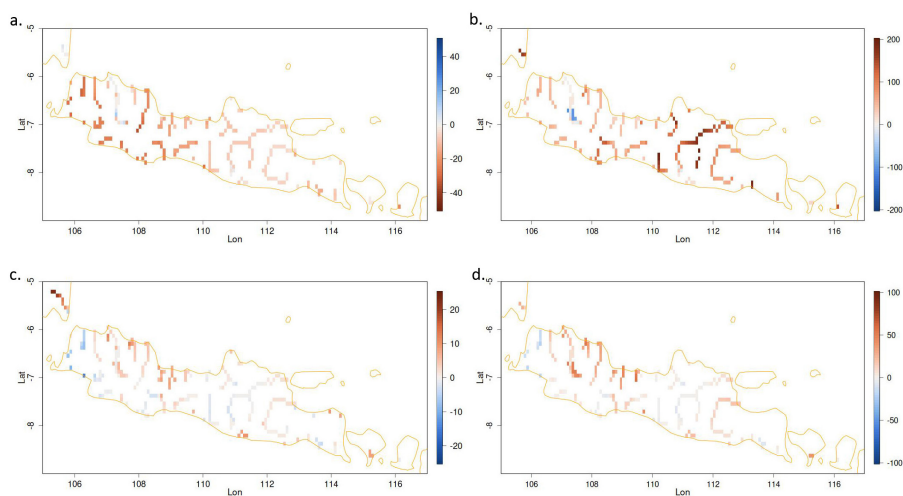


Figure 5. Similar to Fig. 3, but now for the Java region

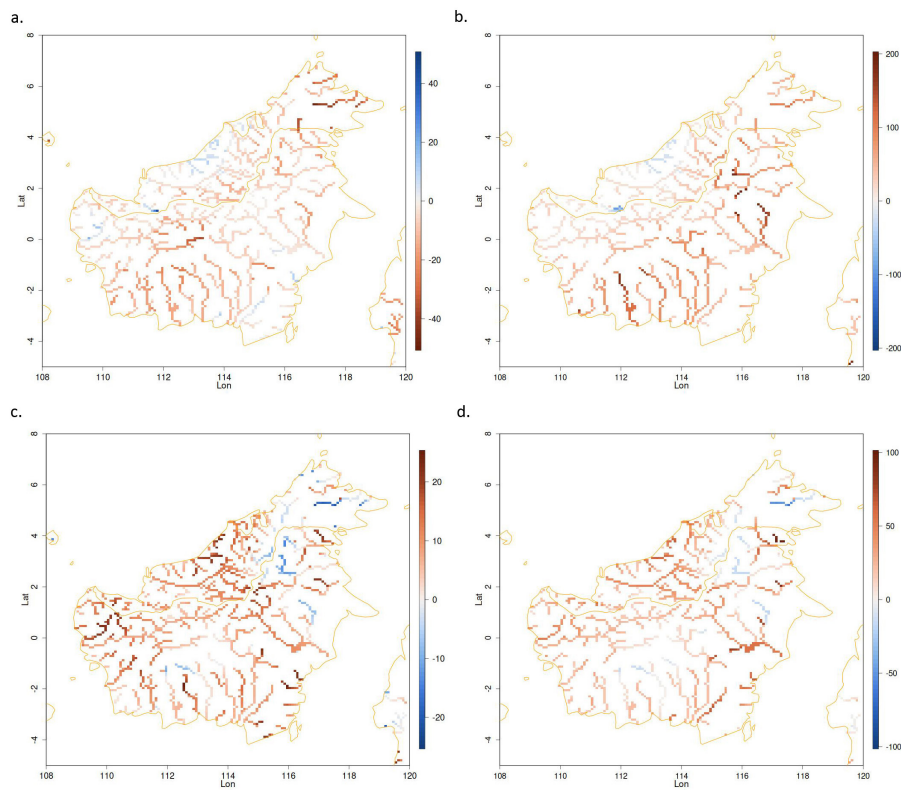


Figure 6. Similar to Fig. 3, but now for the Borneo region



Table 1. List of rainfall related extreme climate indices computed in this study. The indices are calculated annually

Index ID	Index name	Index definition	Unit
CDD	Maximum length of dry spell	The largest number of consecutive days where rainfall is less than 1mm	d
CDD5D*	number of CDD >5 days	Number of CDD periods with more than 5days per time period	n
CWD	Maximum length of wet spell	The largest number of consecutive days where rainfall is at least 1mm	d
CDW5D*	Number of CWD >5 days	Number of CWD periods with more than 5days per time period	n
R10mm	Number of heavy rainfall days	The number of days where rainfall is at least 10 mm	d
R20mm	Number of very heavy rainfall days	the number of days where rainfall is at least 20 mm	d
Rx1day	Maximum daily rainfall	Highest one day precipitation amount	mm
Rx5day	Maximum 5-days rainfall	Highest five day precipitation amount	mm
R5day50mm*	Number of 5 days heavy precipitation periods	The number of 5 day periods with precipitation totals greater than 50 mm	n
R95pTOT	Precipitation percent due to R95p days	The ratio of the cumulative rainfall at wet days with RR > RR95percentile to the total rainfall	%
SDII	Simple daily intensity index per time period	The ratio of annual total rainfall to the number of wet days	mm/day

** not derived from the ETCCDI climate indices*